33rd Annual International Conference of the IEEE EMBS
Boston, Massachusetts USA, August 30 - September 3, 2011

# Atrial Fibrillation Detection using Time-Varying Coherence Function and Shannon Entropy

J. Lee, *Member, IEEE,* D. McManus and K. Chon, *Senior Member, IEEE*

***Abstract*—We introduce a novel method for automatic detection of Atrial Fibrillation (AF) using time-varying coherence functions (TVCF) and Shannon Entropy (SE). The TVCF is estimated by the multiplication of two time-varying transfer functions (TVTFs). Two TVTFs are obtained using two adjacent data segments with one data segment as the input signal and the other data segment as the output to produce the first TVTF; the second TVTF is produced by reversing the input and output signals. The detection algorithm was tested on RR interval time series derived from two databases: the MIT-BIH Atrial Fibrillation (AF) and the MIT-BIH normal sinus rhythm (NSR). The MIT-BIH database contains a variety of short and long AF beats from 25 subjects and the MIT-BIH NSR database consists of only normal sinus rhythms from 18 subjects. Using the receiver operating characteristic curves from the combination of TVCF and SE, we obtained the accuracy of 97.49%, sensitivity of 97.41% and specificity of 97.54% for the MIT-BIH AF database. Furthermore, the specificity of the MIT-BIH NSR database was 100%.**

## I. Introduction

Atrial fibrillation is the most common sustained dysrhythmia worldwide. Over 2.3 million Americans are currently diagnosed, and the prevalence of AF is increasing with the aging of the U.S. population [1]. Through its association with increased risk for heart failure, stroke and mortality, AF has a profound impact on the longevity and quality of life of a growing number of people [2-3]. Although new AF treatment strategies have emerged over the last decade, a major challenge facing clinicians and researchers is the paroxysmal which is difficult to detect because it is short lasting and intermittent. Thus, there is a pressing need to develop methods for accurate AF detection including paroxysmal rhythms. This technology has important clinical applications for pre- and post-treatment detection of AF. For these reasons, the importance of developing new AF detection technologies has been emphasized.

Many algorithms have been developed to detect AF and can be categorized as being based on 1) P-wave detection or 2) RR interval (RRI) variability [4-12]. AF detection based on P-wave absence, has not gained a wide acceptance because determination of the P-wave fiducial point localization is challenging especially for Holter monitoring applications. Indeed, for Holter monitoring, it is difficult to find uncontaminated RR intervals due to motion and noise artifacts which can confound the accuracy of P-wave detection. Subsequently, many studies have used variability of RR interval time series instead [8-12]. Specifically, the aim is to quantify markedly increased beat-to-beat variability RR interval time series in AF. Consequently, most algorithms show higher sensitivity and specificity values than the methods that screen for the absence of P-wave. However, most of these RR intervals methods are based on comparing the density histogram of the data segment with previously-compiled standard density histogram of RR segments during AF using the Kolmogorov-Smirnov test [12]. A main disadvantage of this method is that it requires storage of large amounts of histogram data and threshold values of various characteristics of AF.

In this paper, we used our previously-developed time-varying coherence function (TVCF) approach [16] to discriminate between AF and nonfibrillatory cardiac rhythms. Note that Sarraf et al. [13] have previously used a time-invariant coherence function approach to discriminate between AF and non-AF rhythms with good results. To account for nonstationary dynamics of AF as well as to capture transitions from AF to sinus rhythms, Lovett and Ropella [14] have used a spectrogram approach. However, this study was not intended for AF detection; hence its accuracy value is not known. Further, because the spectrogram does not provide the best time- and frequency-resolutions, its ability to find the transition between AF and normal sinus rhythms is not optimal.

In general, higher time- and frequency-resolutions offered by the parametric over nonparametric approaches are well documented [15]. Hence, our autoregressive moving average (ARMA) model-based TVCF offers higher time and frequency resolutions than nonparametric counterparts. Specifically, an ARMA model-based time-varying transfer function (TVTF) is calculated between two adjacent data segments with one data segment as the input and the other as the output signal. We then reverse the input and output signals and compute the second TVTF, and then multiply two TVCFs to obtain TVCF [16]. Our underlying hypothesis for the use of TVCF approach is that if the two adjacent segments are normal sinus rhythms (NSRs), the resultant TVCF will have values close to one throughout the entire frequency ranges. However, if either or both segment(s) partially or

Manuscript received April 15, 2011. This work was funded in part by the office of Naval Research work unit N00014-08-1-0244.

J. Lee and K. Chon are with the Department of Biomedical Engineering, Worcester Polytechnic Institute, MA 01609 USA (corresponding author to provide phone: 508-831-4114; fax: 508-831-4121; e-mail: jinseok@wpi.edu, kichon@wpi.edu).

D. McManus is with the Cardiology Division, Departments of Medicine and Quantitative Health Sciences, University of Massachusetts Medical Center, Worcester, MA 01605 USA (e-mail: mcmanusd@ummhc.org).

fully contains AF, the coherence values will decrease significantly lower than one at the time instant AF occurs. Finally, to increase the accuracy of our AF detection, we combined TVCF results with Shannon entropy (SE).

## II. Methods

### A. MIT-BIH Database

We used two databases consisting of the MIT-BIH AF and the MIT-BIH NSR. The AF database contains 25 ECG recordings with a total of 299 AF episodes. Each ECG recording is approximately 10 hours in duration. For all databases we used RR interval series. The data sets 4936 and 5091 were excluded from our study due to incorrect AF annotation. The NSR database contains 18 ECG recordings, and each recording is approximately 24 hours. The NSR database does not contain any AF episodes; hence, it is useful for evaluation of the specificity value of AF detection.

### B. Time-Varying Coherence Function (TVCF)

To demonstrate the use of the TVTF in obtaining the TVCF, we first define the TVCF via the nonparametric time-frequency spectra as:

$$|\gamma(t,f)|^2 = \frac{|S_{xy}(t,f)|^2}{S_{xx}(t,f)S_{yy}(t,f)} = \frac{|S_{yx}(t,f)|^2}{S_{yy}(t,f)S_{xx}(t,f)} \quad (1)$$

where $S_{xy}(t,f)$ and $S_{yx}(t,f)$ represent the time-frequency cross-spectrum, and $S_{xx}(t,f)$ and $S_{yy}(t,f)$ represent the auto spectra of the two signals $x$ and $y$, respectively. Specifically, the second term is the coherence function when $x$ is considered as the input and $y$ as the output. Similarly, the third term in Eq. (1) is the coherence function when $y$ is considered as the input and $x$ as the output. For a linear TV system with $x$ as the input and $y$ as the output, TVTF in terms of time-frequency spectra can be obtained as

$$H_{x\to y}(t,f) = \frac{S_{xy}(t,f)}{S_{xx}(t,f)} \quad (2)$$

where $H_{x\to y}(t,f)$ is the TVTF from the input $x$ to the output $y$ signal. Similarly, for a linear TV system with $y$ as the input and $x$ as the output, the TVTF can be obtained as

$$H_{y\to x}(t,f) = \frac{S_{yx}(t,f)}{S_{yy}(t,f)} \quad (3)$$

Thus, time-varying magnitude $|\gamma(t,f)|^2$ is obtained by multiplying the two transfer functions,

$$\left|H_{x\to y}(t,f)H_{y\to x}(t,f)\right| \quad (4)$$

Given the relationship of (4), a high resolution TVCF can be obtained from a ARMA model:

$$y(n) = -\sum_{i=1}^{P_1} a(n,i)y(n-i) + \sum_{j=0}^{Q_1} b(n,j)x(n-j) + e(n) \quad (5\text{-}1)$$

$$x(n) = -\sum_{i=1}^{P_2} \alpha(n,i)x(n-i) + \sum_{j=0}^{Q_2} \beta(n,j)y(n-j) + e'(n) \quad (5\text{-}2)$$

where (5-1) represents *y(n)* as the output and *x(n)* as the input. Similarly, (5-2) represents *x(n)* as the output and *y(n)* as the input. Given the ARMA models of (5), the two transfer functions of (4) can be obtained as [16]

$$H_{x\to y}(n,e^{jw}) = \frac{B(n,e^{jw})}{A(n,e^{jw})} = \frac{\sum_{l=0}^{Q_1} b(n,j)e^{-jwl}}{1+\sum_{i=1}^{P_1} a(n,i)e^{-jwi}}$$

$$H_{y\to x}(n,e^{jw}) = \frac{\beta(n,e^{jw})}{\alpha(n,e^{jw})} = \frac{\sum_{l=0}^{Q_2} \beta(n,j)e^{-jwl}}{1+\sum_{i=1}^{P_2} \alpha(n,i)e^{-jwi}} \quad (6)$$

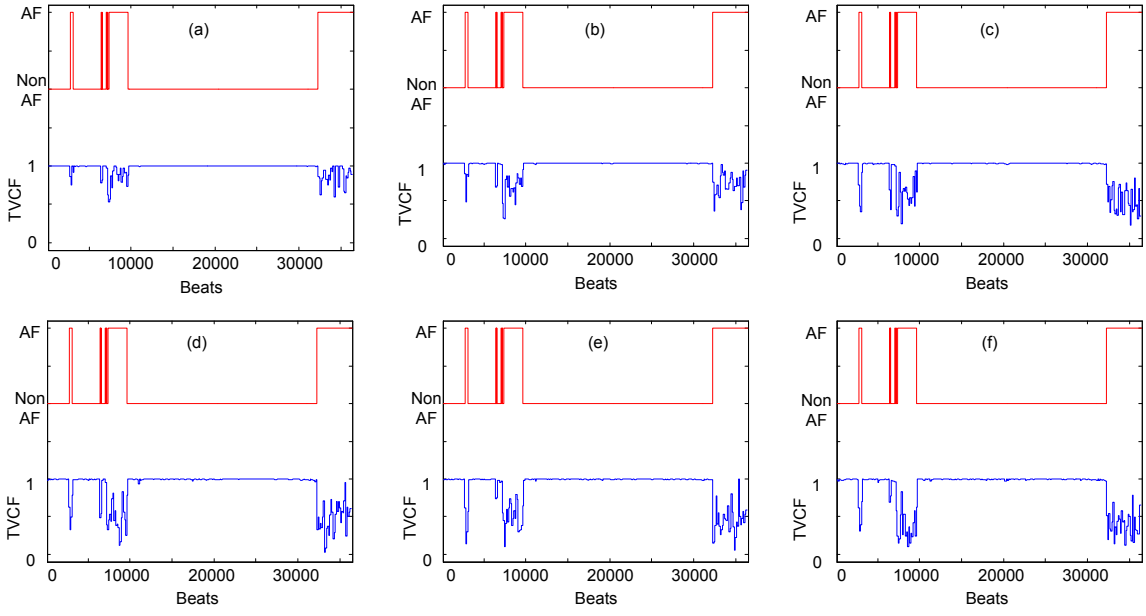


Fig. 1. TVCF at different frequency according to each beat from subject 7910 of the MIT-BIH AF database. (a) frequency at 0.09Hz, (b) frequency at 0.17Hz, (c) frequency at 0.25Hz, (d) frequency at 0.33Hz, (e) frequency at 0.41Hz and (f) frequency at 0.48Hz

Finally, we obtained TVCF by multiplying the two transfer functions as described in (6). For the parameter estimation, we used the time-varying optimal parameter search (TVOPS) criterion [17], as it has been shown to be accurate when applied to diverse physiological signals [18-19]. In all cases, the TVOPS has been shown to be more accurate than the AIC, minimum description length (MDL) and the fast orthogonal search criterion [18-19].

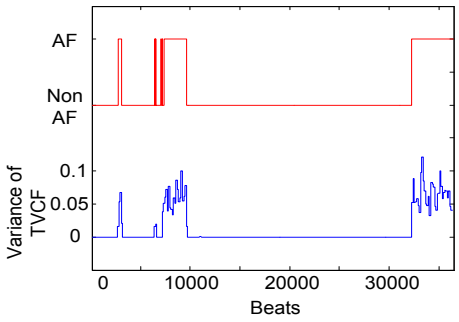


Fig. 2. Frequency variances of TVCF at each beat and True AF annotation from subject 7910 of the MIT-BIH AF database

### C. *Frequency Variability of TVCF for AF Detection*

For AF detection, we formulate two adjacent beat segments with the length of *seg* using the following ARMA models:

$$S_{i+1:i+seg}(n) = -\sum_{i=1}^{P_1} a(n,i)S_{i+1:i+seg}(n-i) + \sum_{j=0}^{Q_1} b(n,j)S_{i+seg+1:i+2\cdot seg}(n-j) + e(n)$$

$$S_{i+seg+1:i+2\cdot seg}(n) = -\sum_{i=1}^{P_1} \alpha(n,i)S_{i+seg+1:i+2\cdot seg}(n-i) + \sum_{j=0}^{Q_1} \beta(n,j)S_{i+1:i+seg}(n-j) + e'(n) \quad (7)$$

where $S_{i+1:i+seg}(n)$ and $S_{i+seg+1:i+2\cdot seg}(n)$ are two adjacent RR interval time series from the $(i+1)^{th}$ to the $(i+seg)^{th}$ and from the $(i+seg+1)^{th}$ to the $(i+2\cdot seg)^{th}$, respectively. By substituting (7) into (6), the two transfer functions are obtained, and the TVCF is finally yielded by multiplication of the two TVCFs. In order to validate the formulation of AF detection, we calculated TVCF using ARMA (5,5) with the first order Legendre function for the subject 7910 of the MIT-BIH AF database. We used a 128 beat segment, which is then shifted by 128 beats. We used a 64 point FFT, which results in the frequency resolution of 0.0156 Hz. Fig. 1 shows the resultant TVCFs at 5 different frequencies out of the 32 possible frequencies. For example, Figs. 1(a)-1(e) correspond to frequencies at 0.09, 0.17, 0.25, 0.33, 0.41 and 0.48 Hz, respectively. Note that with higher frequencies, the TVCF values tend to have lower values during AF. Thus, for each time instant or each beat, we calculate the variance of TVCF values, termed the frequency variations (FV) among all 32 frequencies. Fig. 2 shows the FV of TVCF at each beat with the true AF annotation for the subject 7910 taken from the MIT-BIH AF database. As shown in Fig. 2, this approach results in an accurate detection of the time onset of AF and the transition to NSR.

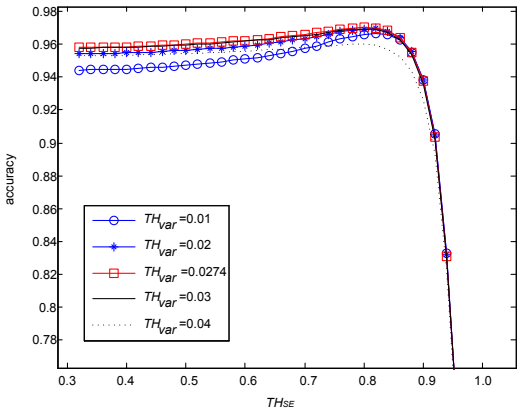


Fig. 3. Accuracy according to $TH_{var}$ and $TH_{SE}$. The highest accuracy is 0.9749 when $TH_{var} = 0.0274$ and $TH_{SE} = 0.78$.

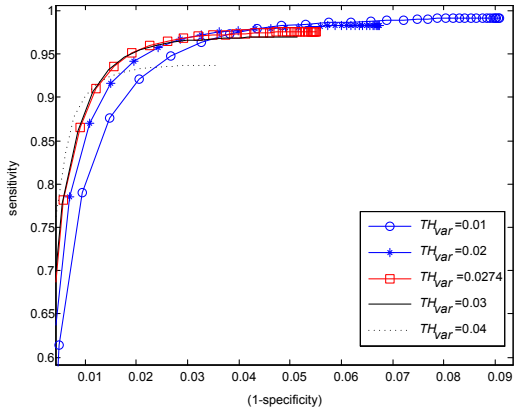


Fig. 4. ROC curves (sensitivity vs (1-specificity)) according to different $TH_{var}$ and $TH_{SE}$. The sensitivity and specificity is 0.9741 and 0.9754, respectively, when the accuracy is 0.9749.

### D. *Shannon Entropy Combination*

The FV-TVCF may cause false negatives and false positives when premature or ectopic beats occur. Thus, we combined the FV-TVCF with Shannon Entropy (SE), which characterizes information complexity. The SE was one of the most powerful tools for AF detection as it is designed to characterize randomness of a signal [8].

### E. *Detector Optimization*

The condition for AF detection is now given by a simple logical AND condition:

- If (FV-TVCF $\geq TH_{var}$) AND (SE $\geq TH_{SE}$), then classify it as AF. Else classify it as non-AF

For the FV-TVCF, we can shift a segment by segment length and compare two adjacent segments. For SE, we shift a segment by one beat. ROC analyses are used to find $TH_{var}$, $TH_{SE}$ and *seg* for optimum sensitivity and specificity. In summary, the algorithm parameters considered for this optimization problem are:

- Segment length *seg* for FV-TVCF varied from 32 to 128. (segment length for SE is constant with 128)
- $TH_{var}$ varied from 0 to 0.1 at interval of 0.0001
- $TH_{SE}$ varied from 0 to 1 at interval of 0.01

We can now define a 3-element vector of algorithm parameters $\boldsymbol{P}_{opt} = [seg, TH_{var}, TH_{SE}]$. The vector parameter can now be varied according to the ranges defined above. For each particular value of the vector $\boldsymbol{P}_k$, we find the number of True Positives ($\mathrm{TP_k}$), True Negatives ($\mathrm{TN_k}$), False Positives ($\mathrm{FP_k}$) and False Negatives ($\mathrm{FN_k}$). We use the sensitivity $\mathrm{TP_k}/(\mathrm{TP_k}+\mathrm{FN_k})$, specificity $\mathrm{TN_k}/(\mathrm{TN_k}+\mathrm{FP_k})$ and accuracy $(\mathrm{TN_k}+\mathrm{TP_k})/(\mathrm{TN_k}+\mathrm{TP_k}+\mathrm{FP_k}+\mathrm{FN_k})$ on the MIT-BIH AF database. To find $\boldsymbol{P}_{opt}$, we first fixed *seg* to 128 and found the optimal $TH_{var}$ and $TH_{SE}$. We repeated the procedure by changing *seg* to 32 and 64. After finding $\boldsymbol{P}_{opt}$, we applied the same parameters to MIT-BIH NSR database.

## III. Results

Fig. 3 shows the accuracy values according to different $TH_{var}$ and $TH_{SE}$ on the MIT-BIH AF database. The segment length *seg* was 128, and the highest accuracy was 0.9749 when $TH_{var} = 0.0274$ and $TH_{SE} = 0.78$. Fig. 4 shows the ROC curves (sensitivity vs (1-specificity)) according to different $TH_{var}$ and $TH_{SE}$. The sensitivity, specificity and accuracy are 0.9741, 0.9754 and 0.9749, respectively. Using this approach, we repeated the same procedure by changing *seg*. We found that the accuracy values were 0.8788 and 0.9571 for *seg*=32 and *seg*=64, respectively. In summary, the vector parameter $\boldsymbol{P}_{opt}$ providing the highest accuracy was found as [128,0.0274,0.78], and we achieved a sensitivity of 97.41%, a specificity of 97.54% (accuracy of 97.49%) for the MIT-BIH AF database. In addition, we applied the optimal parameters to the MIT-BIH NSR database, and achieved the specificity of 100%. A comparison to the recently published algorithms on the MIT-BIH AF and MIT-BIH NSR databases is presented in TABLE I. As shown, our proposed algorithm provides the best accuracy for both databases.

TABLE I
COMPARISON OF RECENT ALGORITHMS ON THE MIT-BIH AF DATABASE AND THE MIT-BIH NSR DATABASE

| Methods | MIT-BIH AF database | | MIT-BIH NSR database |
|---|---|---|---|
| | sensitivity (%) | specificity (%) | specificity (%) |
| Our Proposed Algorithm | 97.41 | 97.54 | 100 |
| Dash et al [8] | 94.4 | 95.1 | 99.7 |
| Tateno and Glass [11] | 94.4 | 97.2 | *(not reported)* |
| Huang et al [12] | 96.1 | 98.1 | 97.9 |
| Logan and Healey [10] | 96.0 | 89.0 | *(not reported)* |
| Kikillus et al [9] | 94.4 | 93.4 | 96.9 |

## IV. Conclusion

In this paper, we presented a novel method for AF detection. The accuracy values were 97.49% and 100% on the MIT-BIH AF and the MIT-BIH NSR databases, respectively. The most attractive feature of TVCF is that it can be used to find the AF onset and transition to NSR. Our method is applicable for a Holter system and can be real-time realizable.

## References


[1] A. S. Go, E. M. Hylek, K. A. Phillips *et al.*, "Prevalence of diagnosed atrial fibrillation in adults: national implications for rhythm management and stroke prevention: the AnTicoagulation and Risk Factors in Atrial Fibrillation (ATRIA) Study," *JAMA,* vol. 285, no. 18, pp. 2370-5, May 9, 2001.

[2] I. Hajjar, and T. A. Kotchen, "Trends in prevalence, awareness, treatment, and control of hypertension in the United States, 1988-2000," *JAMA,* vol. 290, no. 2, pp. 199-206, Jul 9, 2003.

[3] T. S. Tsang, G. W. Petty, M. E. Barnes *et al.*, "The prevalence of atrial fibrillation in incident stroke cases and matched population controls in Rochester, Minnesota: changes over three decades," *J Am Coll Cardiol,* vol. 42, no. 1, pp. 93-100, Jul 2, 2003.

[4] M. Fukunami, T. Yamada, M. Ohmori *et al.*, "Detection of patients at risk for paroxysmal atrial fibrillation during sinus rhythm by P wave-triggered signal-averaged electrocardiogram," *Circulation,* vol. 83, no. 1, pp. 162-9, Jan, 1991.

[5] G. Opolski, P. Scislo, J. Stanislawska *et al.*, "Detection of patients at risk for recurrence of atrial fibrillation after successful electrical cardioversion by signal-averaged P-wave ECG," *Int J Cardiol,* vol. 60, no. 2, pp. 181-5, Jul 25, 1997.

[6] M. Budeus, M. Hennersdorf, C. Perings *et al.*, "[Detection of atrial late potentials with P wave signal averaged electrocardiogram among patients with paroxysmal atrial fibrillation]," *Z Kardiol,* vol. 92, no. 5, pp. 362-9, May, 2003.

[7] D. Michalkiewicz, M. Dziuk, G. Kaminski *et al.*, "[Detection of patients at risk for paroxysmal atrial fibrillation (PAF) by signal averaged P wave, standard ECG and echocardiography]," *Pol Merkur Lekarski,* vol. 20, no. 115, pp. 69-72, Jan, 2006.

[8] S. Dash, K. H. Chon, S. Lu *et al.*, "Automatic real time detection of atrial fibrillation," *Ann Biomed Eng,* vol. 37, no. 9, pp. 1701-9, Sep, 2009.

[9] N. Kikillus, G. Hammer, N. Lentz *et al.*, "Three different algorithms for identifying patients suffering from atrial fibrillation during atrial fibrillation free phases of the ECG," *Comput. Cardiol.,* vol. 34, pp. 801-804, 2007.

[10] B. Logan, and J. Healey, "Robust detection of atrial fibrillation for a long term telemmonitoring system," *Comput. Cardiol.,* vol. 32, pp. 619-622, 2005.

[11] K. Tateno, and L. Glass, "Automatic detection of atrial fibrillation using the coefficient of variation and density histograms of RR and deltaRR intervals," *Med Biol Eng Comput,* vol. 39, no. 6, pp. 664-71, Nov, 2001.

[12] C. Huang, S. Ye, H. Chen *et al.*, "A novel method for detection of the transition between atrial fibrillation and sinus rhythm," *IEEE Trans Biomed Eng,* vol. 58, no. 4, pp. 1113-9, Apr, 2011.

[13] L. S. Sarraf, J. A. Roth, and K. M. Ropella, "Differentiation of atrial rhythms from the electrocardiogram with coherence spectra," *J Electrocardiol,* vol. 35, no. 1, pp. 59-67, Jan, 2002.

[14] E. G. Lovett, and K. M. Ropella, "Time-frequency coherence analysis of atrial fibrillation termination during procainamide administration," *Ann Biomed Eng,* vol. 25, no. 6, pp. 975-84, Nov-Dec, 1997.

[15] S. L. Marple, *Digital Spectral Analysis with Applications*, Englewood Cliffs, NJ: Prentice Hall, 1987.

[16] H. Zhao, S. Lu, R. Zou *et al.*, "Estimation of time-varying coherence function using time-varying transfer functions," *Ann Biomed Eng,* vol. 33, no. 11, pp. 1582-94, Nov, 2005.

[17] R. Zou, H. Wang, and K. H. Chon, "A robust time-varying identification algorithm using basis functions," *Ann Biomed Eng,* vol. 31, no. 7, pp. 840-53, Jul-Aug, 2003.

[18] J. Lee, and K. H. Chon, "Time-varying autoregressive model-based multiple modes particle filtering algorithm for respiratory rate extraction from pulse oximeter," *IEEE Trans Biomed Eng,* vol. 58, no. 3, pp. 790-4, Mar, 2011.

[19] L. Faes, G. Nollo, and K. H. Chon, "Assessment of Granger causality by nonlinear model identification: application to short-term cardiovascular variability," *Ann Biomed Eng,* vol. 36, no. 3, pp. 381-95, Mar, 2008.